

Design of a 90° Overmoded Waveguide Bend*

C. Nantista^o, N. M. Kroll[†] and E. M. Nelson
 Stanford Linear Accelerator Center
 Stanford University, Stanford, CA 94309 USA

Abstract

A design for a 90° bend for the TE₀₁ mode in overmoded circular waveguide is presented. A pair of septa, symmetrically placed perpendicular to the plane of the bend, are adiabatically introduced into the waveguide before the bend and removed after it. Introduction of the curvature excites five propagating modes in the curved section. The finite element field solver YAP is used to calculate the propagation constants of these modes in the bend, and the guide diameter, septum depth, septum thickness, and bend radius are set so that the phase advances of all five modes through the bend are equal modulo 2π. To a good approximation these modes are expected to recombine to form a pure mode at the end of the bend.

I. INTRODUCTION

Some designs for the Next Linear Collider[1] (NLC) transmit power from the source (a klystron or the output of a pulse compressor) to the accelerator structure in the TE₀₁ mode of overmoded circular waveguide in order to have small transmission loss. The waveguide run from the source to the accelerator includes some 90° bends. Ideally these bends would be loss-less.

Two algorithms and some results are presented for the design of one type of overmoded waveguide bend. A curved section of waveguide connects two straight sections as shown in Figure 1a. The curvature in the bend is constant so the waveguide follows a 90° arc with radius of curvature ρ_c between the two straight sections. The cross-section of the waveguide is uniform throughout the curved section, but the cross-section is not simply a circle. The cross-section and radius of curvature ρ_c will be chosen so that the incoming wave propagates through the curved section with negligible mode conversion. This is the principal form of loss considered here. Reflection and wall losses are only considered heuristically. The straight sections are adiabatic tapers from and to circular waveguide.

II. TELEGRAPHIST'S EQUATION

Curvature in overmoded waveguide causes coupling between the straight guide modes. Such coupling is afforded by the generalized telegraphist's equations[2], which have been applied to curved circular guide[3]. In terms of the forward and backward wave amplitudes, a_n[±], these are

$$\frac{da_m^\pm}{dz} = \mp i \sum_n (C_{mn}^\pm a_n^+ + C_{mn}^\mp a_n^-), \quad (1)$$

* Work supported by U.S. Department of Energy contract DE-AC03-76SF00515 and grants DE-FG03-92ER40759 and DE-FG03-92ER40695.

^o Visitor from Department of Physics, UCLA, Los Angeles, CA 90024.

[†] Also from Department of Physics, UCSD, La Jolla, CA 92093.

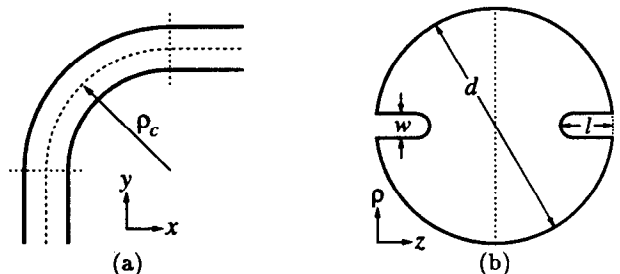


Figure 1. Outer geometry (a) and cross-section (b) of the bend. The cross-section's dashed line is a symmetry plane.

where $C_{mm} = \beta_m$ are the propagation constants and the other C_{mn} involve inner products of the transverse fields.

The power transfer between two modes in a curved section is limited by the difference in their propagation constants. The TE₀₁-TM₁₁ degeneracy presents a problem, so the degeneracy is split by introducing partial septa perpendicular to the bend plane as shown in Figure 1b. The modes can no longer be found analytically, but the β_m can be computed using SUPERFISH[4].

If ρ_c ≫ d/2 then the coupling is weak and the TE₀₁-like mode amplitude varies little along the bend. A small amount of power will beat in and out of the nth coupled mode in an arc length $l_b \simeq 2\pi/|\beta_n - \beta_o|$, where o indicates the TE₀₁-like mode. The interaction with each mode cancels when the relative phase advance is a multiple of 2π. By adjusting the cross-section and ρ_c, the β's are manipulated so that the three propagating modes coupled to first order all beat out at the end of the 90° bend.

This is the approach first taken. However, a compact bend which cannot rely on the above assumption is desired. As the coupling coefficients become comparable to the mode spacings, the beat lengths are altered, and modes coupled to second order may be important. The coupling coefficients C_{mn} are required to verify parasitic mode suppression at the end of the bend. Since the C_{mn} are not easily obtained from the field solver, a different approach was taken.

III. MODES IN CURVED GUIDE

A curved guide can be treated as a portion of a cylindrically symmetric structure. For the 90° bend the structure starts at φ = 0 and ends at φ = π/2. The fields in the waveguide can be decomposed into modes with azimuthal dependence e^{imφ}. In the axisymmetric waveguide paradigm the waves propagate along φ with propagation constant m. Compare this with the phase e^{iβz} for waves propagating along z with propagation constant β in straight waveguides. The curved guide does not close on

itself so there is no requirement that m be an integer.

The finite element field solver YAP[5] is capable of computing the frequencies of the modes of axisymmetric structures for any real m . Non-integral m is allowed. YAP was used to compute dispersion diagrams for curved guide with various cross-sections. One such dispersion diagram is shown in Figure 2. A dispersion diagram for curved guide looks similar to dispersion diagrams for straight guide. However, the simple dispersion formula $\omega^2/c^2 = k_c^2 + \beta^2$ for a straight waveguide containing no media does not apply to curved guide. This can be seen best in figure 2, where the dispersion curves are not parallel lines. A power series of the form

$$\frac{\omega^2}{c^2} = k_c^2 + \alpha_1 \left(\frac{m}{\rho_c}\right)^2 + \alpha_2 \left(\frac{m}{\rho_c}\right)^4 + \dots \quad (2)$$

approximates the dispersion curves well. The cutoff k_c^2 and the coefficients α_i depend on ρ_c and on the cross-section Ω of the guide. When ρ_c is large then $\alpha_1 \cong 1$ and the cutoffs k_c^2 are approximately the same between straight and curved guide with the same cross-section. In the large ρ_c limit the two approaches described in this paper are equivalent.

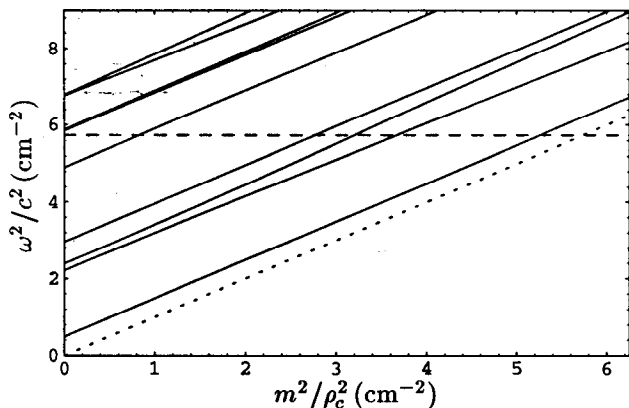


Figure 2. Dispersion diagram of the curved guide for the first design listed in Table 1. The dashed line is the drive frequency 11.424 GHz. The dotted line corresponds to the speed of light along the center of the guide.

IV. SCATTERING AT THE INTERFACE

There is potentially some reflection at the interface between the straight waveguide and the curved waveguide. A generalized scattering matrix \mathbf{S}_i for the propagating modes in the straight and curved guides can be constructed.

As an example, the scattering matrix for the straight-to-curved interface in an overmoded rectangular H-plane waveguide bend was computed using a mode-matching method. Only TE_{n0} modes were considered so the fields are uniform vertically. In the straight guide propagating along y the modes are $E_z \propto \sin(2\pi nx/w)$ where $0 \leq x \leq w$ is the horizontal domain of the waveguide. In the curved guide the modes involve Bessel functions. They are $E_z \propto AJ_m(k\rho) + BY_m(k\rho)$ where $\rho_c - w/2 \leq \rho \leq \rho_c + w/2$

and $k = \omega/c$ is the drive frequency. Note that m is real for propagating modes and imaginary for evanescent modes.

The boundary conditions $E_z = 0$ at $\rho = \rho_c \pm w/2$ yield a characteristic equation for the propagation constants m . Solutions were obtained by numerically integrating Bessel's equations and using a shooting method to match the boundary conditions. This yielded numerical values for m^2 for both propagating ($m^2 > 0$) and evanescent ($m^2 < 0$) modes. The field E_z for each mode was obtained similarly.

The normalized generalized scattering matrix \mathbf{S}_i was computed for an example with $w/\lambda = 1.36$ and $\rho_c/\lambda = 3.87$, where λ is the free space wavelength. There are two propagating modes in the guides. Using 14 modes for the field expansion on each side of the interface, the computed scattering matrix for the interface is

$$\mathbf{S}_i = \begin{bmatrix} 4 \cdot 10^{-5} \angle -8^\circ & 8 \cdot 10^{-4} \angle -2^\circ & 0.982 & 0.190 \\ 8 \cdot 10^{-4} \angle -2^\circ & 8 \cdot 10^{-4} \angle -122^\circ & -0.190 & 0.982 \\ 0.982 & -0.190 & 3 \cdot 10^{-4} \angle -4^\circ & 8 \cdot 10^{-4} \angle -4^\circ \\ 0.190 & 0.982 & 8 \cdot 10^{-4} \angle -4^\circ & 6 \cdot 10^{-4} \angle -82^\circ \end{bmatrix} \quad (3)$$

where $[a_{s1}, a_{s2}, a_{c1}, a_{c2}]^T$ is the incoming wave vector. The wave amplitudes a_{sn} and a_{cn} are for the modes in the straight and curved guides, respectively.

Notice that the reflection amplitude is less than 10^{-3} . If one assumes the reflections are similar for bends with different cross-sections but similar curvature, then reflection at the straight-to-curved interface can be neglected. The reflected power will be negligible as long as resonances are avoided. The principal concern, then, is mode conversion.

V. AROUND THE BEND

The scattering matrix \mathbf{S}_b for a bend over angle ϕ_b can be easily computed given \mathbf{S}_i for the straight-to-curved interface and the propagation constants m_1 and m_2 for the two propagating modes in the curved guide. The example above has $m_1 = 22.85$ and $m_2 = 16.18$. The next mode is evanescent with $m_3 = i11.38$. The transmission coefficient for the (straight guide) fundamental mode for various bend angles ϕ_b was computed. At $\phi_b = 2\pi/(m_1 - m_2) = 0.941$ the transmission is nearly perfect. At this bend angle the two propagating waves in the curved guide arrive at the output end of the bend with the same relative phases they had at the input end of the bend. The propagating field at the output is the same as at the input except for an overall phase, so waves are faithfully transmitted through the bend with no mode conversion.

The evanescent waves at the interfaces have decayed sufficiently in the curved guide so that they can be neglected in the transmission calculations for $\phi_b = 0.941$.

This example leads to the principal design criterion for this type of overmoded waveguide bend: the phases $e^{m_i \phi_b}$ must be identical for all modes propagating in the curved guide. In addition, evanescent modes should be sufficiently above cutoff so that they decay well over the length of the bend, and thus can be neglected.

Table 1
90° Overmoded Waveguide Bends

d (cm)	l (cm)	w (cm)	ρ_c (cm)	m_1	m_2	m_3	m_4	m_5	f_{c6} (GHz)
4.372	0.986	0.465	31.786	72.873	60.873	56.873	52.873	28.874	11.536
4.275	0.971	0.611	36.655	83.867	67.867	63.867	59.867	23.868	11.819
4.358	1.054	0.593	38.754	89.034	73.034	69.034	65.034	25.033	11.579
3.940	0.765	0.476	23.891	53.870	41.870	37.870	33.870	9.871	12.726
4.157	0.904	0.622	33.894	77.212	61.212	57.212	53.212	17.213	12.163

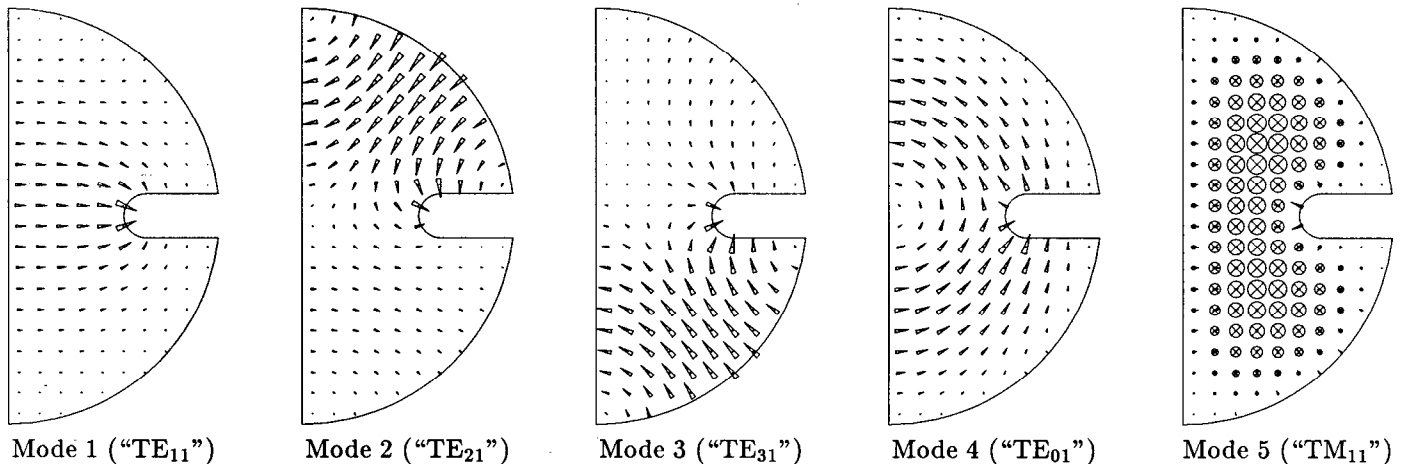


Figure 3. Electric field patterns for the five propagating modes of the first design in Table 1.

VI. 90° BEND DESIGN

Designs for a 90° bend with a cross-section as shown in Figure 1b were computed. The phases $e^{m_i\pi/2}$ for the five lowest propagating modes excited by the incoming wave can be fixed relative to each other by adjusting the four parameters: d , ρ_c , l and w . Propagating modes not excited by the incoming wave (due to symmetry) are neglected. Dispersion diagrams were computed using YAP and the bend parameters were adjusted so that the phases were the same. This corresponds to the propagation constants m_i differing from one another by multiples of 4. The cutoff ($m = 0$) frequency of higher order modes were computed in order to discard designs with more than five propagating modes at 11.424 GHz. Table 1 lists the parameters for five solutions. It also lists the propagation constants for the five lowest modes and the cutoff frequency f_{c6} for the sixth lowest mode.

The cross-section in Figure 1 and the dispersion diagrams in Figure 2 correspond to the first design in Table 1. The field patterns for the propagating modes are shown in Figure 3. At cutoff the field patterns for the modes in curved guide are similar to the corresponding modes in straight guide, but for large m the second and third modes are mixed. This is evident in the field plots and in the dispersion diagram, where it appears that the second and third curves are repelling each other. These modes arise, with the introduction of the septa, from the TE_{21} and TE_{31} modes of circular guide. The incoming wave is similar to the fourth mode, which is a TE_{01} -like mode.

The cutoff frequency for the sixth mode of the first design appears close to cutoff. The estimated propagation constant using the straight guide formula is $m_6 \cong i10.7$

and the decay amplitude over the length of the waveguide is $e^{im_6\pi/2} = 5 \times 10^{-8}$.

VII. FURTHER WORK

Further designs can be found, perhaps with smaller radii of curvature and shorter septa so that the bend will have smaller wall losses and be easier to manufacture.

A variation of the YAP field solver will compute the evanescent modes in curved guide. With these modes a mode-matching algorithm can be employed to calculate the scattering matrix S_i for the straight-to-curved guide interface, and then verify that reflections are negligible and that the design criterion is appropriate.

Calculation of the wall losses through the bend and mode-conversion losses (due to manufacturing errors) also requires knowledge of S_i in order to obtain the mode amplitudes in the bend as well as the evanescent fields near the interface.

VIII. REFERENCES

- [1] R. D. Ruth, "The Development of the Next Linear Collider at SLAC," SLAC-PUB-5729 (1992).
- [2] S. A. Schelkunoff, "Generalized Telegraphist's Equations for Waveguides," *Bell System Technical Journal*, **31**, pp. 784-801, July, 1952.
- [3] S. P. Morgan, "Theory of Curved Circular Waveguide Containing an Inhomogeneous Dielectric," *B.S.T.J.*, **37**, pp. 1209-1251, Sept., 1957.
- [4] K. Halbach and R. F. Holsinger, *Particle Accelerators* **7**, 213 (1976).
- [5] E. M. Nelson, "A Finite Element Field Solver for Dipole Modes," SLAC-PUB-5881, 1992 *Linear Accelerator Conference Proceedings*, pp. 814-816.